Title: The multi-Siglec inhibitor AL009 reprograms suppressive macrophages and activates innate and adaptive tumor immunity

Authors: Sam C. Nalle,* Helen Lam, Ling Leung, Spencer Liang, Daniel Maslyar, Arnon Rosenthal

Affiliation:

Alector, Inc., South San Francisco, CA, USA.

*Corresponding author. Email: Sam.Nalle@alector.com

Abstract:

Sialic acid–binding immunoglobulin-type lectins (Siglecs) are cell surface receptors that regulate innate and adaptive immunity, with inhibitory Siglecs promoting immune tolerance. In the tumor microenvironment, overexpression of sialic acid glycans exploits inhibitory Siglec signaling, leading to a cancer-permissive phenotype. AL009 is an engineered Siglec-9-Fc fusion molecule that functions as a sialic acid trap and reprograms suppressive macrophages to activate an anti-tumor immune response. AL009 treatment of human myeloid-derived suppressor cells (MDSCs), an in vitro model of tumor-associated macrophages (TAMs), resulted in an increase in proinflammatory cytokines and chemokines, changes in cell surface markers, and potent relief of T cell inhibition in a co-culture assay. In syngeneic mouse tumor models, AL009 engineered with a mouse Fc (AL009m) reduced tumor growth as a monotherapy and in combination with the checkpoint inhibitor anti–PD-L1. In addition, AL009m synergized with the tumor-targeting therapy anti-TRP1 to reduce lung nodules in the B16-F10 intravenous model. Pharmacodynamic

marker analysis in syngeneic and humanized mouse tumor models supported an AL009 mechanism of action based on reprogramming TAMs and enhanced T cell activation. Future clinical studies are warranted to further elucidate the safety and efficacy of AL009.

One Sentence Summary: Preclinical data for AL009 support investigation of this therapeutic for treatment of cancers rich in suppressive macrophages.

Main Text:

INTRODUCTION

Sialic acid–binding immunoglobulin-like lectins (Siglecs) are immune regulatory molecules that interact with sialic acid residues in the glycocalyx to modulate innate and adaptive immune response (*1-3*). Inhibitory Siglecs, such as Siglec-3, -5, -7, -9, and -10, contain an immunoreceptor tyrosine-based inhibition motif (ITIM) that recruits tyrosine phosphatases (such as SHP1 and SHP2) involved in dampening the immune response to maintain homeostasis (*1, 2, 4, 5*). This is particularly important for recognition of self and resolution of inflammation (*6*). However, some tumors have exploited this process by overexpressing sialic acid ligands on the tumor cell surface to engage inhibitory Siglecs and evade immune detection, thus promoting an immunosuppressive, cancer-permissive phenotype (*1, 5, 7, 8*). Disrupting the signaling between immune-inhibitory Siglecs and their sialic acid ligands on hypersialylated cancer cells could confer a therapeutic benefit, making both Siglecs and their sialic acid ligands attractive targets for cancer immunotherapies (*2, 8, 9*).

44 Siglecs are expressed on various immune cells but predominantly on myeloid cells, including
45 macrophages and myeloid-derived suppressor cells (MDSCs) (*2, 5*). The immunoregulatory
46 activity of macrophages, whether proinflammatory or immunosuppressive, can change
47 depending on the chemokines, cytokines, and enzymes in the surrounding environment, with
48 tumor-associated macrophages (TAMs) being primarily immunosuppressive due to the nature of
49 the tumor microenvironment (TME) (*5, 10-13*). TAMs are not only influenced by the TME but
50 also contribute to the immunosuppressive signaling therein by releasing anti-inflammatory
51 chemokines and cytokines, such as IL-10 and TGF-β, which ultimately lead to T cell inactivation
52 (*10, 13*). Cell surface markers can be used to monitor the current immunomodulatory status of
53 macrophages; MHC-II, CD80, and CD86 are increased on proinflammatory macrophages, while
54 suppressive macrophages display elevated CD163 and CD206 (*5, 13-15*). TAM infiltration into
55 tumors has been associated with worse prognosis, particularly when high levels of Siglecs are
56 displayed (*16, 17*).

57 Targeted therapeutics designed to reprogram TAMs from an immunosuppressive to a
58 proinflammatory phenotype are currently being investigated (*11*). Thus far, antibodies against
59 macrophage receptor with collagenous structure (MARCO), the leukocyte immunoglobulin-like
60 receptor B (LILRB) family, Clever-1, and P-selectin glycoprotein ligand-1 (PSGL-1), as well as
61 CD40 agonists, have all shown potential in converting TAMs into proinflammatory effectors
62 (*18-22*). Interferon gamma (IFNɣ) has also shown potential to skew macrophages towards a
63 proinflammatory phenotype (*15, 18, 23*). The immunosuppressive characteristic of inhibitory
64 Siglecs along with their expression on TAMs make them ideal targets to modulate macrophage
65 function. However, since multiple inhibitory Siglecs are expressed on TAMs, broad targeting is
66 required to effectively interrupt immunosuppressive Siglec signaling (*4, 5*).

67 Here, we present data on AL009, an engineered multi-Siglec inhibitor that functions as a sialic
68 acid trap and reprograms suppressive macrophages to activate an anti-tumor immune response.
69 In vitro, AL009 effectively reprograms suppressive macrophages, as demonstrated by changes in
70 cell surface markers as well as increased secretion of proinflammatory cytokines. In animal
71 tumor models, monotherapy with AL009 or combination therapy with AL009 and anti–PD-L1 or
72 anti-TRP1 reduced tumor burden. Taken together, these data support further investigation of
73 AL009 as a targeted immunotherapy across a broad range of tumors high in Siglec-expressing
74 TAMs.

75

76 **RESULTS**

77 **AL009 displays specific blocking between inhibitory Siglecs and their ligands**

78 AL009 is composed of a Siglec-9 extracellular domain (ECD) and an engineered Fc to localize
79 the therapeutic to immune cells and promote cooperative binding of the ECD. Given the
80 redundancy of inhibitory Siglecs, an effective therapeutic would require broad blocking between
81 multiple inhibitory Siglecs and their respective ligands. To assess the degree to which AL009
82 could disrupt Siglec-ligand binding on MDSCs, the binding between Siglec-3, -5, -7, -9, and -10
83 Fc fusion proteins and human MDSCs was quantified in the presence of increasing
84 concentrations of AL009. With all the Siglec Fcs tested, an AL009 dose-dependent decrease in
85 binding was observed, demonstrating a broadly effective blockade of ligand recognition on cells
86 (Fig. 1A). In order to assess specific ligand blockade, a biochemical blocking assay using AL009
87 was established with a glycan array containing over 100 sialic acids. Using this assay format,
88 AL009 blocked binding of known sialic acids recognized by inhibitory Siglecs -3, -5, and -7
89 (Fig. 1B-D). As the binding portion of AL009 is composed of a Siglec-9 ECD, Siglec-9 binding

relative to other inhibitory Siglecs was evaluated side by side using a glycan array. Siglec-9 displayed an extensive sialic acid binding profile compared to other inhibitory Siglecs (Fig. S1), helping to explain the ability of AL009 to block ligands recognized by multiple Siglecs on MDSCs. Overall, these results demonstrate that AL009 possesses the ability to block specific ligand binding of at least 5 inhibitory Siglecs present on myeloid cells.

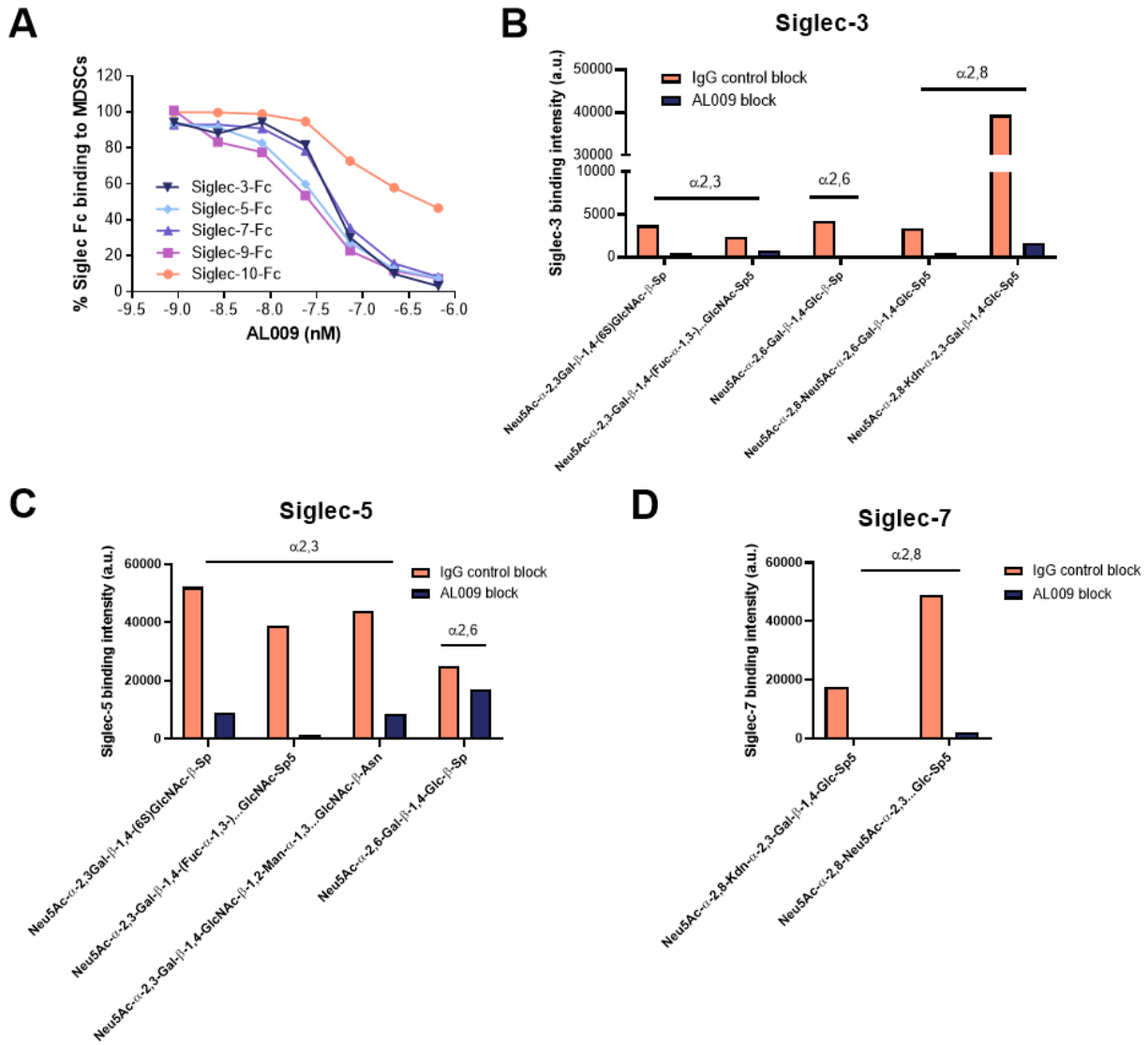

Fig. 1. AL009 blocks binding of inhibitory Siglec receptors and their ligands. (**A**) AL009 blocked binding of Siglec-3, -5, -7, -9, and -10 from binding to MDSCs in a dose-dependent

98 manner. (**B-D**) In a glycan array containing over 100 sialic acids, AL009 blocked Siglec-3, -5,
99 and -7 from binding their respective ligands. Fc, fragment crystallizable; IgG, immunoglobulin
100 G; MDSCs, myeloid-derived suppressor cells; Siglec, sialic acid–binding immunoglobulin-type
101 lectin.

102

103 **AL009 reprograms MDSCs**

104 The phenotypic effect of AL009 blocking recognition between inhibitory Siglecs and their
105 ligands was assessed by incubating MDSCs with AL009 and evaluating cell surface markers,
106 cytokines, and chemokines. AL009 treatment resulted in a dose-dependent increase in immune
107 activation marker CD86 and a dose-dependent decrease in the immunosuppressive macrophage
108 marker CD163, consistent with reprogramming of MDSCs (Fig. 2A, 2B). Further, tumor
109 necrosis factor (TNF) production was increased in a dose-dependent manner (Fig. 2C). In order
110 to gain a greater understanding of the reprogramming effect of AL009 on MDSCs, RNAseq
111 analysis was performed on MDSCs after AL009 treatment. AL009 induced robust expression of
112 cytokines, chemokines, and co-stimulatory molecules compared to isotype control in MDSCs
113 (Fig. 2D).

114 We considered whether the reprogramming effect of AL009 treatment was specific to the
115 Siglec-9 ECD portion of the molecule. To evaluate this, MDSCs were treated with Siglec-3, -5, -
116 7, -9, or -10 ECD-Fc fusions and the reprogramming effect was assessed. The Siglec-9–mIgG
117 fusion resulted in the largest increase in activation markers CD86 and CD40 and the largest
118 reduction in suppressive macrophage markers CD163 and CD206 (Fig. S2). The Siglec-9–mIgG
119 fusion was also the only Siglec-Fc fusion that induced a dose-dependent increase in CCL4
120 production by MDSCs, consistent with reprogramming of these cells (Fig. S3).

121 Next, we examined whether AL009 was able to rescue MDSC suppression of T cells in a co-
122 culture system. MDSCs were treated with ligand-blocking antibodies against Siglec-3, -7, or -9,
123 a combination of all 3 antibodies, or AL009 prior to co-culture with activated T cells. The
124 amount of IFNɣ produced by the T cells was reduced in the presence of MDSCs and was not
125 rescued by any treatment except AL009 (Fig. 2E). In addition to increasing IFNɣ production in T
126 cells, we tested AL009's impact on T cell proliferation. After treatment with increasing
127 concentrations of AL009, T cell proliferation was quantified, with a half maximal effective
128 concentration (EC_{50}) of 1 to 2 nM AL009 (Fig. S4). Overall, AL009 is effective at potently
129 repolarizing MDSCs, resulting in phenotypic changes consistent with a proinflammatory
130 response and relief of T cell inhibition.

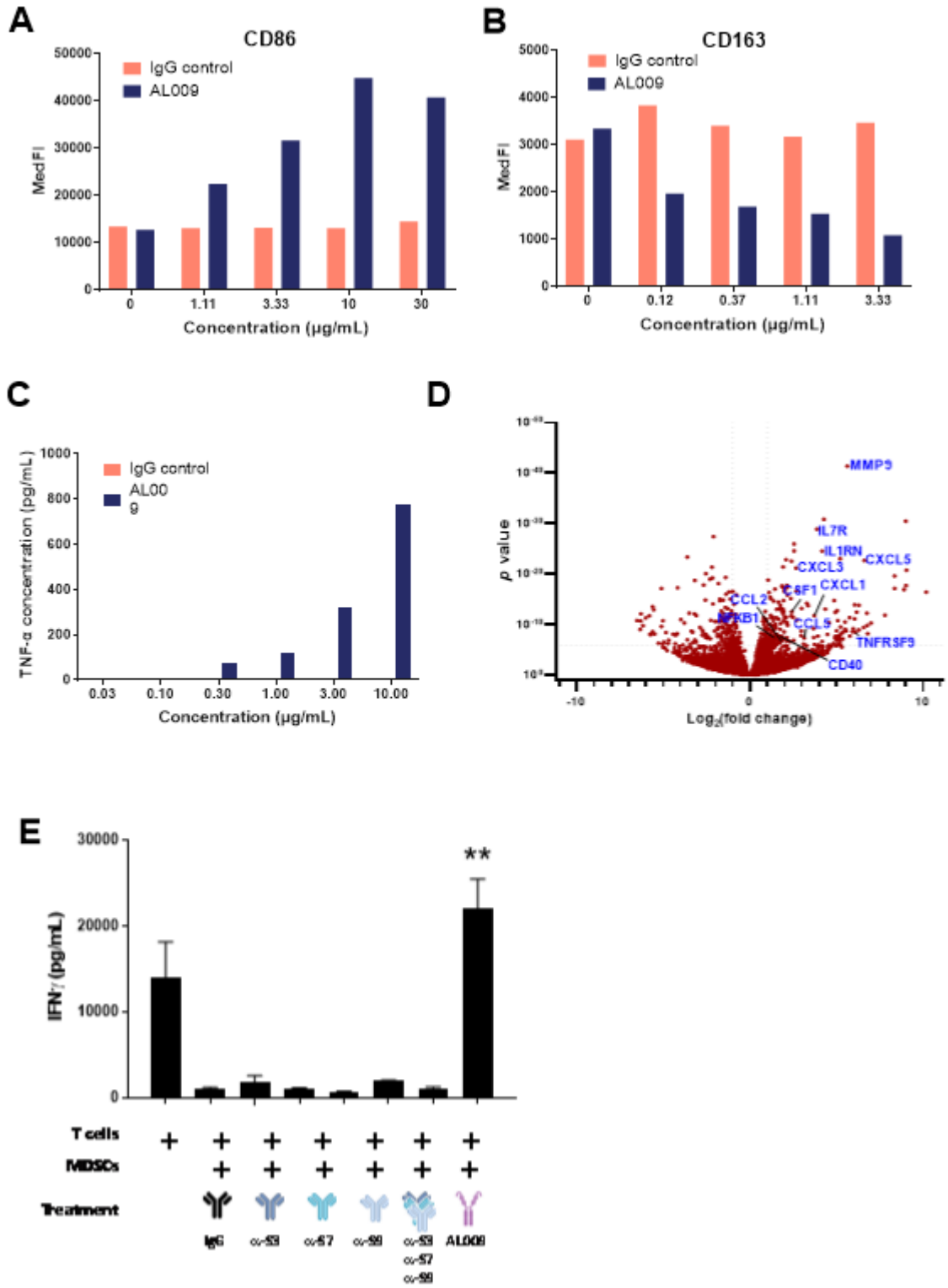

Fig. 2. AL009 repolarizes suppressive MDSCs. AL009 (**A**) enhanced CD86, (**B**) repressed CD163, and (**C**) induced TNF secretion after treatment on MDSCs. (**D**) AL009 treatment of

134 MDSCs led to robust changes in gene expression. (**E**) AL009 rescued T cells suppressed by
135 MDSCs in a co-culture system. Error bars represent standard error of the mean. IFNγ, interferon
136 gamma; IgG, immunoglobulin G; mAbs, monoclonal antibodies; MDSCs, myeloid-derived
137 suppressor cells; MedFI, median fluorescence intensity; Siglec, sialic acid–binding
138 immunoglobulin-type lectin; TNF, tumor necrosis factor. $^{**}p < 0.01$, 2-sided t-test.

139

140 **AL009 activity depends on the ECD and Fc regions**

141 We hypothesized that both the Siglec-9 ECD and engineered Fc regions of AL009 were
142 important for the function of the molecule. To determine the contribution of the Siglec-9 ECD
143 portion of AL009, we first created domain mutation constructs. Production of the chemokine
144 CCL5 was induced with AL009, but that effect was ablated when the Siglec-9 ECD portion of
145 AL009 was deleted (Fig. 3A). Next, the Siglec-9 ECD and Fc fusion portions of AL009 were
146 decoupled, and MDSCs were incubated with plate-bound IgG to engage Fcγ receptors (FcγRs),
147 with or without a soluble AL009 mutant consisting of only the Siglec-9 ECD, then analyzed for
148 TNF production as a marker of MDSC programming (Fig. 3B). FcγR engagement by increasing
149 concentrations of plate-bound IgG induced a low level of TNF that was enhanced by the addition
150 of Siglec-9 ECD (Fig. 3C). We next asked if the Siglec-9 ECD could augment a separate
151 activation signal beyond FcγRs. Soluble anti-TREM1 or anti-TREM2 agonist antibodies were
152 incubated with MDSCs at increasing concentrations in addition to Siglec-9 ECD. Anti-TREM1
153 and anti-TREM2 had very minimal effects on MDSCs alone, but the addition of a fixed amount
154 of Siglec-9 ECD resulted in increased secretion of TNF in combination with TREM1 or TREM2
155 antibodies (Fig. 3D). These results demonstrate that Siglec-9 ECD alone is active and synergizes
156 with an activation signal in order to reprogram MDSCs.

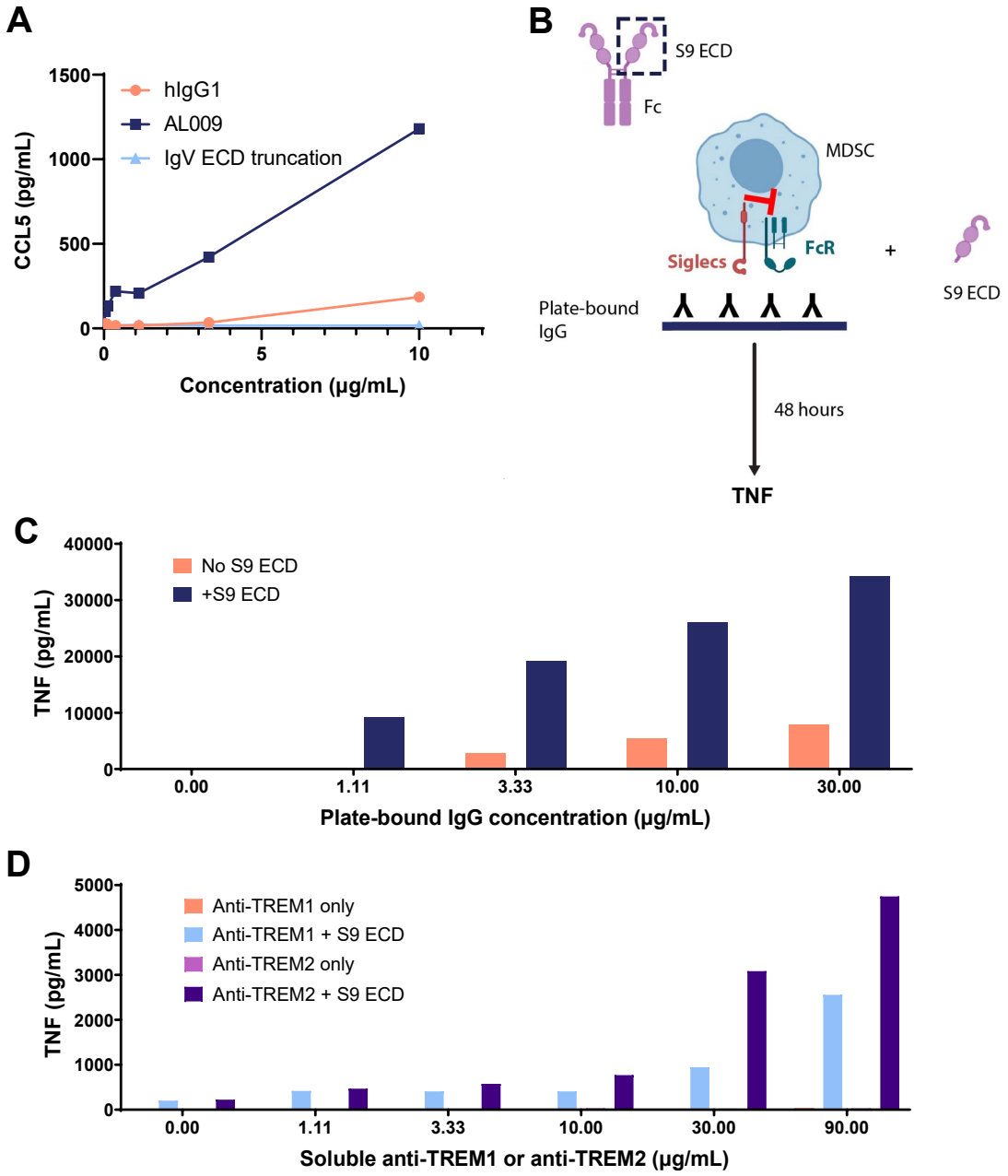

Fig. 3. The Siglec-9 ECD relieves immune suppression in the presence of an activating signal. (**A**) Truncation of the ECD domain of AL009 ablated its ability to induce CCL5. (**B**) Schematic of experimental setup. (**C**) Levels of TNF produced by MDSCs upon IgG cross-linking were increased in the presence of Siglec-9 ECD. (**D**) Levels of TNF produced by MDSCs were not induced by anti-TREM1 or anti-TREM2 alone but were induced when Siglec-9 ECD

163 was present. ECD, extracellular domain; Fc, fragment crystallizable; IgG, immunoglobulin G;
164 MDSCs, myeloid-derived suppressor cells; MedFI, median fluorescence intensity; Siglecs, sialic
165 acid–binding immunoglobulin-type lectins; TNF, tumor necrosis factor.

166

167 The contribution of the Fc portion of AL009 was also investigated. The ability of AL009 to
168 relieve T cell suppression in an MDSC–T cell co-culture assay was greatly reduced when the Fc
169 portion of AL009 was silenced via mutations that ablate binding to FcγRs (Fig. 4A). To further
170 examine the contribution of the Fc portion of AL009 in binding MDSCs, dissociation constants
171 on cells were determined. The dissociation constant for AL009 when incubated with MDSCs
172 was 1.3 nM. However, when non-Fc receptor–expressing cells were used in place of MDSCs,
173 binding was much weaker (Kd = 220 nM). Similarly, when the Fc portion of AL009 was
174 silenced, binding to MDSCs was greatly reduced (Kd = 97 nM). In order to determine which Fc
175 gamma receptors were important for AL009 function, the ability of AL009 to increase CD86
176 expression at the cell surface, as a marker of MDSC reprogramming, was assessed in the
177 presence of antibodies against FcγRIIa, FcγRIIb, or a combination of FcγRIIa and FcγRIIb. The
178 N325S/L328F (NSLF) mutation contained within the Fc portion of AL009 prevents binding to
179 FcγRIIIa and FcγRIIIb; therefore, as expected there was no effect when MDSCs were incubated
180 with an FcγRIII blocking antibody prior to AL009 treatment. FcγRIIa blockade reduced AL009
181 activity, while FcγRIIb had no effect. Consistent with these results, the combination of FcγRIIa-
182 and FcγRIIb-blocking antibodies was equivalent to FcγRIIa blockade alone (Fig. 4B). Taken
183 together, these results suggest FcγRIIa is necessary for AL009 activity on MDSCs.

184

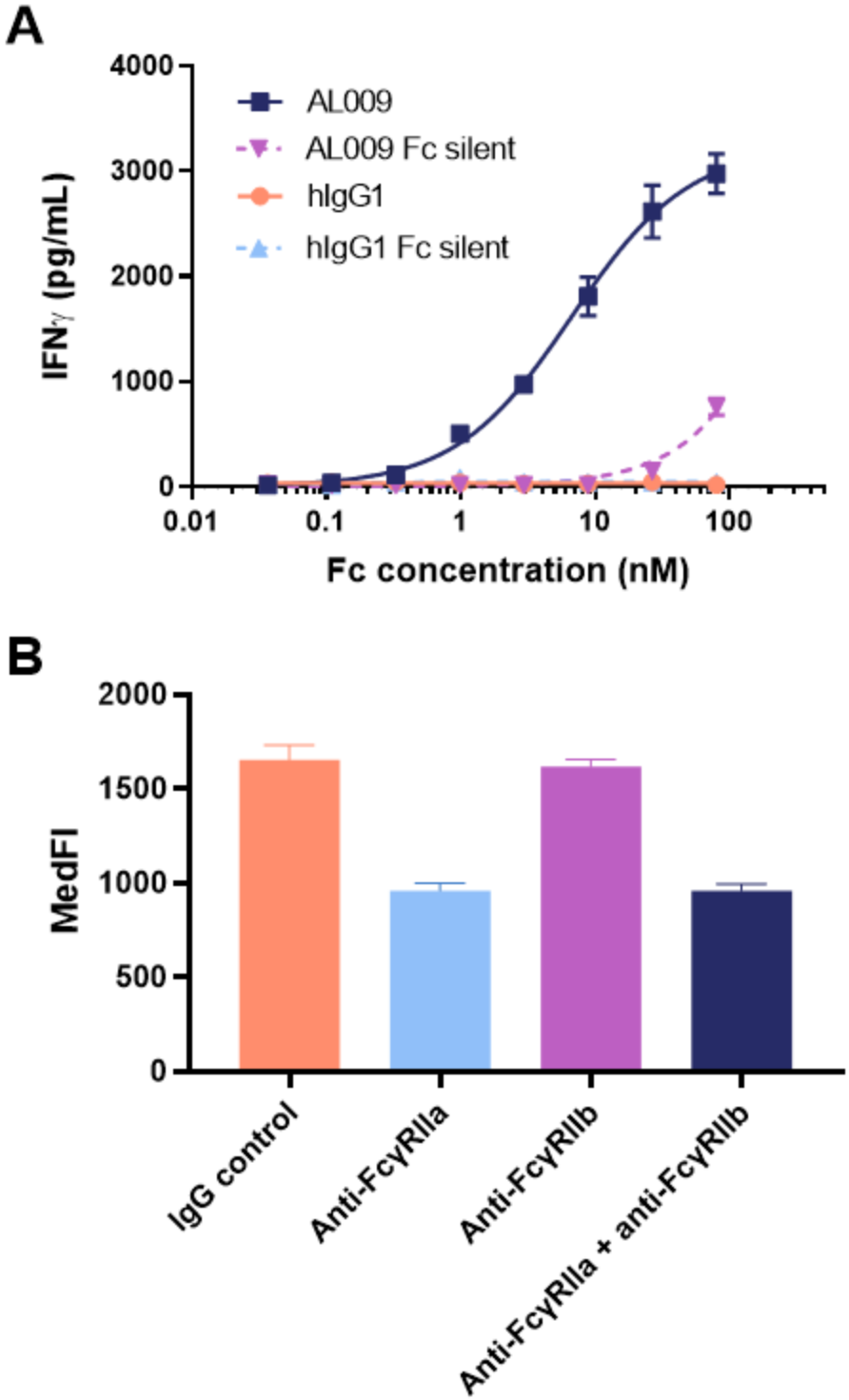

185

186 **Fig. 4. AL009 activity requires Fc receptor interactions.** (**A**) While AL009 was able to

187 reverse MDSC suppression and lead to higher levels of IFNγ compared to control, AL009 Fc

188 silent was not able to elevate IFNɣ to the same extent. (**B**) FcɣRIIa was required for functional
189 activity of AL009 on MDSCs. Data are shown as mean ± SEM. Fc, fragment crystallizable;
190 IFNɣ, interferon gamma; IgG, immunoglobulin G; MDSC, myeloid-derived suppressor cell;
191 MedFI, median fluorescence intensity; SEM, standard error of the mean.

192

193 **AL009 preferentially binds myeloid cells**

194 In whole human blood, binding of AL009 to a variety of immune cell subsets, including
195 monocytes, granulocytes, B cells, natural killer (NK) cells, T cells, and platelets, was assessed.
196 AL009 preferentially bound monocytes compared to the other immune cell subsets tested (Fig.
197 5A). To further elucidate cell subsets that are preferentially bound by AL009, donor blood
198 samples were used to compare AL009 binding to monocytes, macrophages, and MDSCs. The
199 highest binding observed was between AL009 and MDSCs, followed by non-activated M0
200 macrophages, and then classically activated M1 macrophages (Fig. 5B).

201 AL009m, a mouse reactive surrogate for AL009 containing a mouse Fc, was created to assess the
202 activity of AL009 in vivo. A biodistribution study was performed with AL009m by fluorescently
203 labeling the molecule and then injecting it intravenously in mice. AL009m accumulation was
204 higher than the isotype control in macrophage-rich mouse tissue samples, such as liver and
205 spleen, while no difference between AL009m or isotype control was seen in other tissues, such
206 as heart and lung (Fig. 5C-5F). The results from both the whole human blood binding study and
207 biodistribution study provide evidence that AL009 preferentially binds myeloid cells both in
208 vitro and in vivo.

209

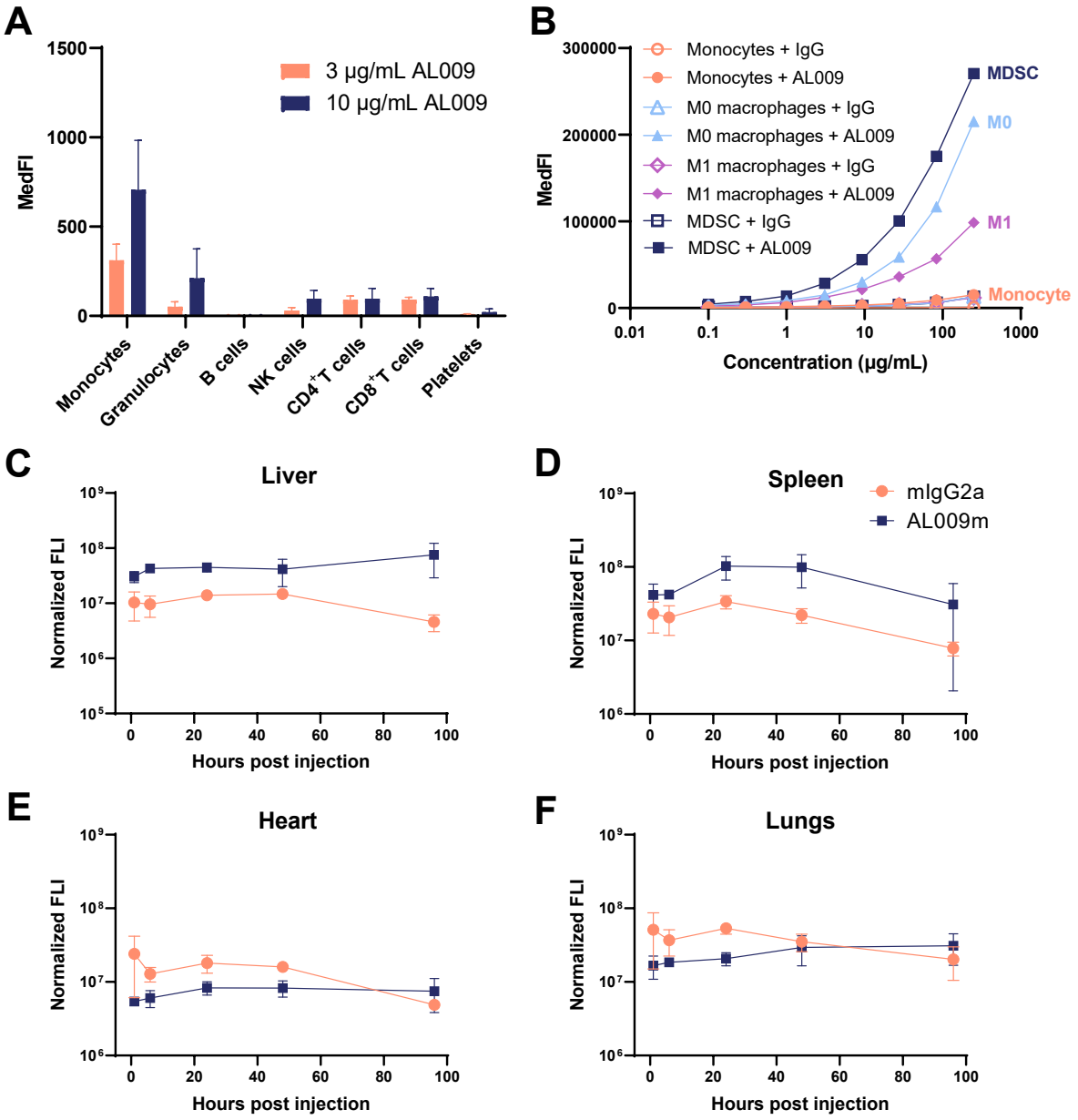

Fig. 5. **AL009 preferentially binds myeloid cells.** (**A**) In whole human blood, AL009 preferentially bound monocytes over granulocytes, B cells, NK cells, T cells, and platelets. (**B**) AL009 preferentially bound MDSCs over other myeloid subsets, including M0 and M1 macrophages and monocytes. (**C-F**) In a biodistribution study in mice, AL009m accumulated in macrophage-rich tissues, such as liver and spleen (n = 3 mice per timepoint). Error bars represent

216 standard error of the mean. FLI, fluorescence intensity; IgG, immunoglobulin G; MDSC,
217 myeloid-derived suppressor cell; MedFI, median fluorescence intensity; NK, natural killer.
218

219 **AL009m demonstrates anti-tumor activity in mouse syngeneic tumor models**

220 Several syngeneic mouse tumor models were used to assess the anti-tumor efficacy of AL009m
221 in vivo. As a monotherapy, AL009m was tested in the E0771 triple negative breast cancer model.
222 Tumor volume was reduced and survival improved with AL009m treatment compared to isotype
223 control (Fig. 6A, 6B). To assess the impact of AL009m in combination with other therapies, the
224 B16-F10 intravenous injection model in combination with anti-TRP1 was utilized. In this model,
225 anti-TRP1 induces macrophage-mediated antibody-dependent cellular phagocytosis (ADCP) and
226 antibody-dependent cellular cytotoxicity (ADCC) of B16-F10 melanoma cells (*24*). Combination
227 treatment with AL009m and anti-TRP1 resulted in a significant reduction of lung nodules
228 compared to anti-TRP1 and isotype control (Fig. 6C). These results demonstrate that AL009m
229 can enhance ADCP/ADCC in vivo. To test the combination of AL009 with checkpoint
230 inhibitors, anti–PD-L1 was utilized along with AL009m in the MC38 and E0771 models. In both
231 models, anti–PD-L1 alone was not significantly different than isotype control, whereas
232 combination treatment with AL009m led to a significant reduction in tumor volume (Fig. 6D,
233 6E). Taken together, these efficacy results demonstrate that AL009m is active as a monotherapy
234 and in combination with an agent that induces ADCP/ADCC and the representative checkpoint
235 inhibitor anti–PD-L1.

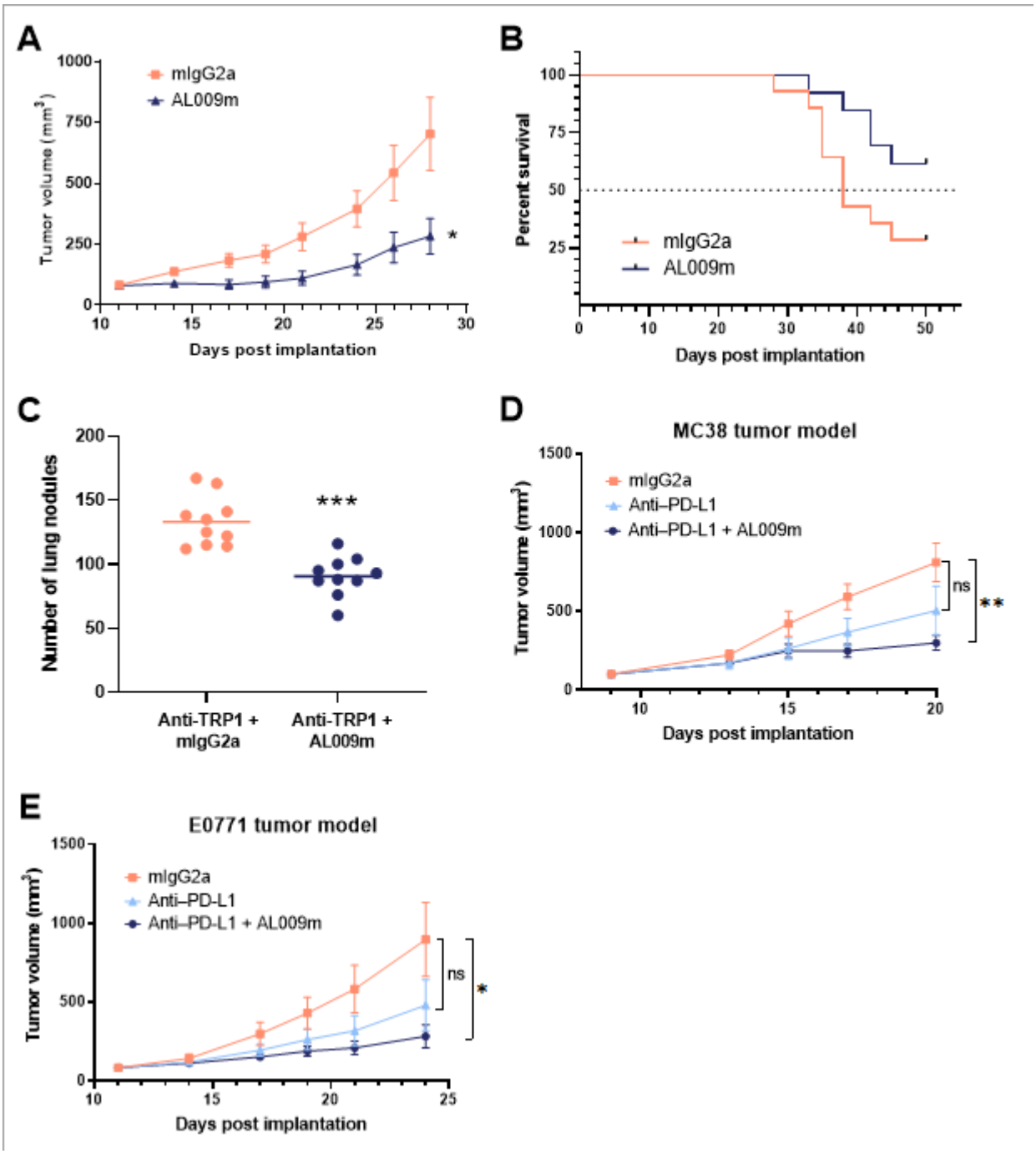

Fig. 6. **AL009m demonstrated anti-tumor activity in multiple mouse syngeneic tumor models.** (**A**) In the E0771 breast cancer model, AL009m treatment resulted in a significant reduction in tumor volume as well as (**B**) increased survival. (**C**) In the intravenous B16-F10 tumor model, combination treatment with anti-TRP1 and AL009 resulted in reduced lung

241 nodules. Line at mean. (**D**) In the MC38 tumor model, combination treatment with AL009m and
242 anti–PD-L1 resulted in reduced tumor volume. (**E**) In the E0771 breast cancer model,
243 combination treatment with AL009m and anti–PD-L1 showed a synergistic effect. (D-E) Data
244 are shown as mean ± SEM. *$p < 0.05$, **$p < 0.01$, ***$p < 0.001$, 2-sided t-test. IgG,
245 immunoglobulin G; ns, not significant.

246

247 **Pharmacodynamic markers show enhanced immune activation in the tumor and spleen**
248 **following AL009 treatment**

249 To evaluate the pharmacodynamic effect of AL009m in the context of a tumor, spleen and tumor
250 samples from the E0771 mouse tumor models were analyzed by flow cytometry following
251 treatment with AL009m alone or in combination with anti–PD-L1. As a monotherapy, AL009m
252 treatment resulted in a significant decrease in Ly6C$^+$ cells, as a percentage of CD11b$^+$ cells,
253 indicating a decrease in MDSCs in tumor tissue (Fig. 7A). In spleen samples, an increase in
254 HLA-DR with AL009m treatment signaled activation of splenic macrophages (Fig. 7B). Further,
255 following AL009m treatment, there was a concurrent increase in activated CD4$^+$ cells in the
256 spleen, as measured by an enhanced percentage of CD69$^+$ cells (Fig. 7C). There was also an
257 increase in activated CD8$^+$ cells induced by AL009m that was further enhanced by anti–PD-L1
258 treatment, indicating a synergistic effect (Fig. 7D). In addition to the effects observed in the
259 tumor and spleen, AL009m also induced a dose-dependent increase in surface CD86 on
260 circulating monocytes (Fig. S5), similar to what was observed on human MDSCs following
261 AL009 treatment (Fig. 2A). The pharmacodynamic effect of AL009 was further evaluated in a
262 humanized mouse tumor model. In this humanized model, immunodeficient mice were engrafted
263 with human CD45$^+$ stem cells, implanted with a human A375 tumor weeks later, and treated

264 with AL009 approximately 2 weeks post implantation. Flow cytometry was used to analyze
265 tumor and spleen samples. Treatment with AL009 significantly decreased surface CD163 on
266 TAMs and splenic macrophages (Fig. 7E, 7F), demonstrating an in vivo reprogramming effect
267 consistent with the in vitro reprogramming observed with human MDSCs.

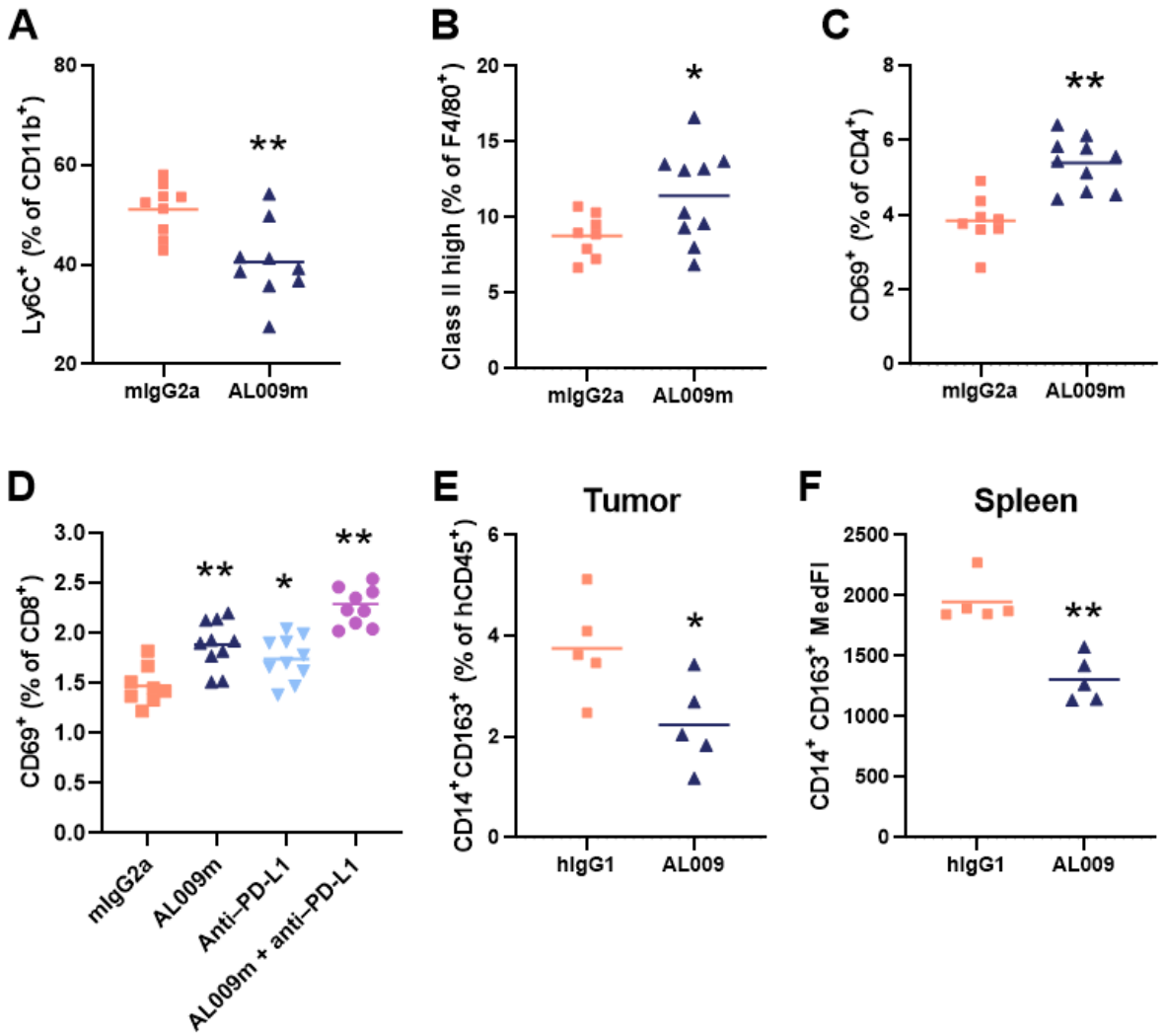

268

269 **Fig. 7. Pharmacodynamic biomarker data provides evidence that AL009m repolarizes**
270 **myeloid cells and activates T cells in vivo.** In the E0771 mouse tumor model, AL009m
271 treatment (**A**) decreased MDSCs in tumor tissue as shown by a decrease in Ly6C^{+} cells, (**B**)
272 activated macrophages in spleen tissue as shown by increased Class II high cells, and (**C**)

activated $CD4^+$ T cells, as shown by an increase in $CD69^+$ cells. (**D**) $CD8^+$ T cells were also increased with anti–PD-L1 treatment alone or in combination with AL009m treatment. (**E-F**) In a humanized mice tumor model, AL009 treatment decreased levels of the pharmacodynamic biomarker CD163, a marker for suppressive M2 macrophages, in the tumor and spleen. IgG, immunoglobulin G; MDSC, myeloid-derived suppressor cell; MedFI, median fluorescence intensity. Mean is shown. $*p < 0.05$, $**p < 0.01$, 2-sided t-test.

DISCUSSION

The current state of immunotherapy offers significant promise to treat cancer; however, while up to half of all patients may be eligible for treatment with immunotherapy, less than 15% derive clear benefit (*25*). TAMs heavily influence the TME and may comprise up to 50% of tumor mass, which creates barriers to anti-tumor immunity and may underlie the resistance of some patients to checkpoint inhibitors such as anti-PD1, anti–PD-L1, and anti-CTLA4 (*26*). Consequently, an aspect of cancer immunotherapy drug development has shifted focus to targeting the suppressive myeloid cells associated with tumors. There are currently TAM-targeting therapeutics under investigation which aim to either deplete TAMs, block recruitment of macrophages to the tumor, or reprogram TAMs to a proinflammatory phenotype (*26, 27*). Depletion and blocking recruitment of macrophages disregard the anti-tumor potential of creating reprogrammed, proinflammatory macrophages in the TME (*27*). Reprogramming TAMs to a proinflammatory phenotype results in stimulation of cytotoxic T cells and tumor regression in preclinical studies (*26*). Therapeutics aiming to reprogram TAMs may be effective as a monotherapy or in synergy with checkpoint inhibitors (*26, 28*). As a TAM-reprogramming therapeutic, AL009 provides two potential avenues for enabling immunotherapeutic activity: as a

296 monotherapy to drive macrophage modulation of the TME towards a more immune-responsive
297 environment, and in combination with checkpoint inhibitors to disrupt inherent immune-
298 mediated inhibition of the adaptive immune response. AL009 therefore represents a novel, multi-
299 functional therapeutic that has capacity for interrupting multiple negative regulatory signals in
300 TAMs with significant potential for treating cancer.

301 With its Siglec-9 ECD and engineered Fc region, AL009 targets immune cells to widely block
302 inhibitory signaling from Siglec receptors, leading to reprogramming of suppressive
303 macrophages. Siglecs are responsible for regulating immune homeostasis, with inhibitory Siglecs
304 playing a critical role in dampening immune responses (*4, 8*). The data from our experiments
305 confirm the ability of the Siglec-9 ECD of AL009 to bind sialic acid ligands of not only Siglec-9
306 but also other inhibitory Siglecs, thus broadly blocking immune-inhibitory Siglec–sialic acid
307 interactions. The disruption of this interaction allows anti-tumor activation signaling to proceed
308 (Fig. 8). The engineered Fc portion of AL009 facilitates localization to immune cells and
309 cooperative binding with the Siglec-9 ECD results in increased activity on innate immune cells.
310 (Fig. 8).

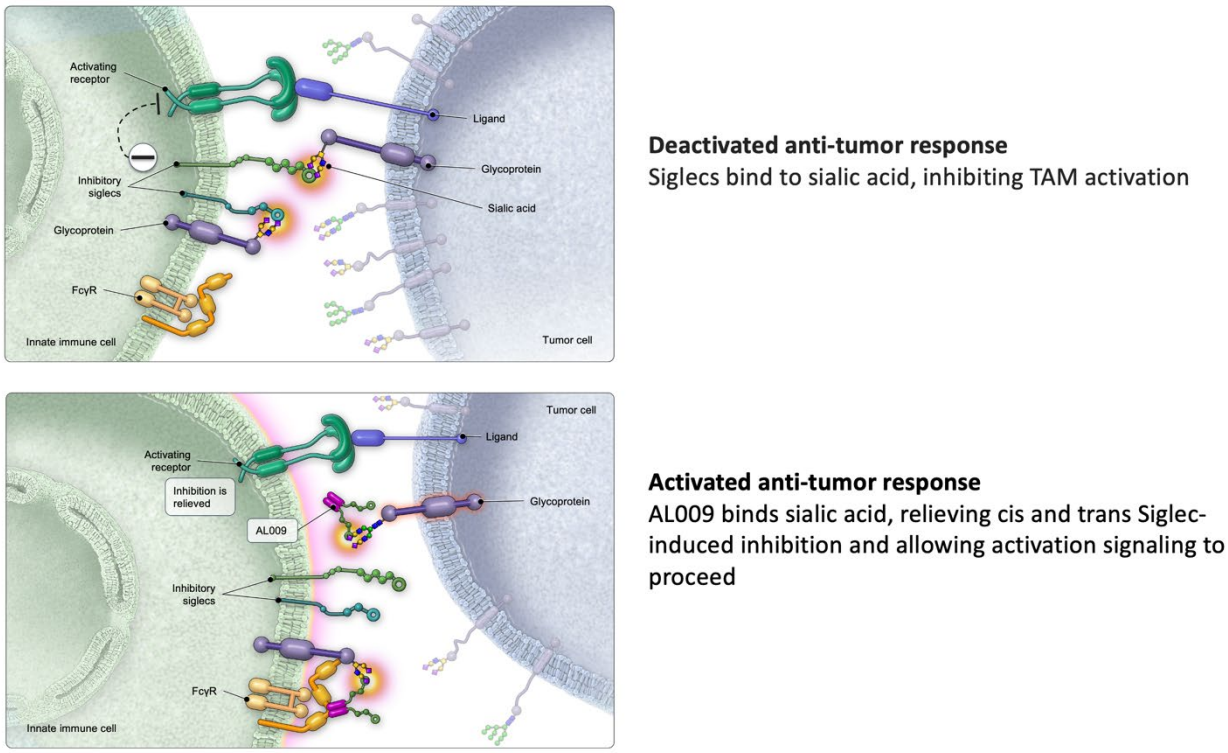

Fig. 8. AL009 mechanism of action. AL009 consists of an extracellular Siglec domain and an engineered Fc portion for immune cell targeting. The Siglec portion of AL009 binds sialic acid ligands in a cis or trans fashion, relieving Siglec-mediated immune suppression.

Overall, AL009 is a differential approach to test the therapeutic hypothesis that TAM reprogramming is an effective method of generating an anti-tumor effect in humans. Thus far, pre-clinical studies have not identified any significant toxicology signals. In addition, serum and immune cell pharmacodynamic biomarkers have been identified, and immunohistochemistry companion diagnostic development is underway. Taken together, these preclinical results support clinical testing of the safety and efficacy of AL009.

324 **MATERIALS AND METHODS**

325 **Study design**

326 The objective of this study was to evaluate the activity of AL009 in vitro and in mouse tumor
327 models. Experiments were designed to elucidate the role of AL009's Siglec-9 ECD and its
328 engineered Fc region, as well as its interactions with and impact on human myeloid cells.
329 Additionally, AL009 pharmacodynamics and efficacy were tested in mouse models.

330 **Animals and reagents**

331 C57BL/6 mice harboring a BAC-expressing human Siglec-3, -7, and -9 (hSiglec BAC Tg) were
332 generated and maintained by Alector. Expression of human Siglecs was confirmed by flow
333 cytometry. Mice were maintained by crossing Tg^{het} mice with wildtype (WT) C57BL/6 mice,
334 and all mice used in studies were Tg^{het} mice. Anti–PD-L1 was produced at Alector based on a
335 reported sequence. Siglec Fcs and isotype control antibodies were produced at Alector unless
336 otherwise stated. In mouse syngeneic tumor studies, a chimeric form of AL009 was produced
337 with a mouse IgG2a Fc (AL009m). huNOG-EXL humanized mice were purchased from Taconic
338 Biosciences (Germantown, NY) and housed at Alector.

339 **Cell binding competition assay with AL009**

340 MDSCs were generated from healthy human donors by differentiation of $CD14^+$ monocytes
341 isolated using a RosetteSep human monocyte enrichment kit (STEMCELL Technologies). In
342 order to generate MDSCs, $CD14^+$ monocytes were cultured for 7 days in Roswell Park Memorial
343 Institute (RPMI) media containing 10-ng/mL human granulocyte-macrophage colony-
344 stimulating factor (GM-CSF) and 10-ng/mL human IL-6 (PeproTech). For cell binding
345 competition with AL009, MDSCs were incubated with titrating amounts of AL009, followed by

346 incubation with Siglec-3, -5, -7, -9, or -10 mouse IgG1 Fc fusion molecules. Bound Siglec-3, -5,
347 -7, -9, and -10 Fcs were assessed by detecting with an anti-mouse IgG-specific secondary
348 (Thermo Fisher) and analyzed via flow cytometry (BD Biosciences).

349 **Glycan array**

350 We assessed binding to a library of 300 glycan structures for Fc fusion proteins sourced from a
351 commercial vendor (R&D Systems) composed of a fusion of Siglec-3, -5, -7, -9, -10, or -15
352 ECDs with a human IgG1 Fc. Siglec fusion proteins and control human IgG1 were assessed for
353 glycan binding on the Glycan-300 (RayBiotech). The staining and analysis were performed as a
354 service by RayBiotech using the manufacturer's protocol. Briefly, the recombinant proteins were
355 incubated with the glycan array for 2 to 3 hours, followed by detection with anti-hIgG biotin and
356 streptavidin-Cy3. Samples were read and fluorescence was normalized across samples. For
357 blocking experiments, AL009 and mIgG1 or mIgG1 alone were applied first before incubation
358 with Siglec Fcs and human IgG.

359 **MDSC stimulation and RNAseq analysis of MDSCs treated with AL009**

360 MDSCs were treated with AL009 for 48 hours at 37° C and cell surface markers and cytokine
361 production were analyzed via flow cytometry and LEGENDplex (Biolegend), respectively. For
362 RNAseq analysis, MDSCs were treated with 10 µg/mL of AL009 for 24 hours. Cells were
363 harvested and pelleted, followed by resuspension in RLT buffer (Qiagen). RNA was extracted
364 with the RNeasy Plus Microkit (Qiagen). Illumina compatible libraries were created using
365 Lexogen QuantSeq 3' mRNA-Seq Library Prep Kit FWD and sequenced on a Nextseq P2.

366 **MDSC–T cell co-culture**

367 The activity of AL009 was evaluated alongside several different functional Siglec antibodies in a
368 MDSC–T cell co-culture assay. MDSCs were harvested and co-cultured with autologous $CD8^+$ T
369 cells in the presence of Dynabeads Human T-activator CD3/CD28 (Thermo) and either a Siglec-
370 Fc fusion or antibodies. Proliferation via carboxyfluorescein succinimidyl ester (CFSE, Thermo
371 Fisher) dilution and cytokine production via LEGENDplex were assessed after 3 to 5 days.

372 **MDSC stimulation with plate-bound IgG and anti-TREM1/anti-TREM2**

373 MDSCs were stimulated with plate-bound human IgG1 with or without 10-µg/mL Siglec-9 ECD
374 co-incubation for 48 hours followed by analysis of TNF production (Meso Scale Discovery).
375 Separately, MDSCs were stimulated with anti-TREM1 or anti-TREM2 agonistic antibodies with
376 or without Siglec-9 ECD for 48 hours followed by analysis of TNF production.

377 **Fcγ receptor blockade**

378 MDSCs were incubated with the 10-µg/mL FcγRIIa (clone IV.3)- or FcγRIIb (clone 2B6)-
379 blocking antibodies alone or in combination for 30 minutes on ice, followed by treatment with
380 3.3-µg/mL AL009 for 24 hours at 37° C and analysis of cell surface markers by flow cytometry.

381 **Specific binding of AL009**

382 For peripheral immune cell binding specificity, healthy human blood was incubated with AF647-
383 labeled AL009 using SiteClick reagents (Thermo Fisher) followed by analysis via flow
384 cytometry. For myeloid binding, healthy human monocytes from peripheral blood, M0
385 macrophages differentiated from human monocytes with 50-ng/mL human M-CSF, M1
386 macrophages differentiated from human monocytes with 50-ng/mL M-CSF, 100-ng/mL LPS
387 (InvivoGen), and 50-ng/mL IFNγ (PeproTech), or MDSCs, were incubated with AF647-labeled
388 AL009 followed by analysis via flow cytometry.

389 **Biodistribution of AL009**

390 Female C57BL/6 mice bearing established subcutaneous MC38.NCI.TD1 murine colon
391 carcinoma were injected intravenously with 10-mg/kg AF647-labeled AL009m. Ex vivo
392 fluorescence imaging (FLI) using the IVIS Spectrum imaging system was performed on liver,
393 spleen, heart, and lungs collected from each mouse at 1, 6, 24, 48, and 96 hours post injection.
394 Three animals were imaged per time point.

395 **Effect of AL009 in mouse models**

396 The MC38 and B16-F10 cell lines were purchased from ATCC. The E0771 cell line was
397 purchased from MI Bioresearch. Female S3/7/9 Tg mice that were 7 to 12 weeks old were
398 implanted with MC38 or E0771 cells subcutaneously in the flank region at a density of 1.0×10^5
399 or 4.0×10^5 cells per mouse, depending on the model. When tumors reached an average volume
400 of ~100 mm^3, mice were randomized into treatment groups and dosing was initiated. Mice
401 received intraperitoneal injections of 10- to 20-mg/kg AL009m or isotype control with or
402 without 3-mg/kg anti–PD-L1 twice per week for 3 weeks. Tumors were measured twice per
403 week with calipers. For the B16-F10 intravenous model, 1.5×10^5 B16-F10 cells were
404 administered via intravenous injection. Mice were treated with 27-µg/mouse anti-TRP1
405 (BioXCell) on day 1 in addition to 10-mg/kg AL009m or isotype control on days 1, 4, 7, 10, and
406 13. A satellite group of animals was dosed only with control antibodies, and several mice in this
407 group were euthanized every 2 days starting on day 9 to assess lung nodules. When the satellite
408 group reached 50 to 100 lung nodules, the remaining experimental groups were euthanized for
409 analysis. Statistical testing was performed by 2-way Student's t-test.

410 **Pharmacodynamic biomarkers**

411 Siglec-3/7/9 BAC Tg mice were implanted with E0771 tumors and randomized for treatment as
412 described above. The mice received intraperitoneal 20-mg/kg AL009m or isotype control on
413 days 0, 4, and 7, and were sacrificed on day 8. Splenic and tumor tissues were mechanically
414 dissociated and passed through a 70-μm filter to obtain single-cell suspensions. Peripheral blood
415 was treated with ammonium-chloride-potassium (ACK) lysis buffer to lyse red blood cells and
416 washed with phosphate-buffered saline (PBS). Cell surface markers on immune cell subsets were
417 analyzed by flow cytometry.

418 For pharmacodynamic analysis of humanized mice, 14- to 16-week-old female huNOG-EXL
419 mice were implanted with A375 melanoma cells subcutaneously in the flank region at a density
420 of with 3.0×10^6 cells per mouse. When tumors reached an average volume of 200 to 400 mm^3,
421 mice received intraperitoneal injections of 10-mg/kg AL009 or isotype control on days 0 and 3
422 and were sacrificed 24 hours later. Cell surface markers on immune cells subsets were analyzed
423 by flow cytometry.

424 **Statistical analyses**

425 Statistical analysis was performed using GraphPad Prism v9. Data are displayed as mean ± SEM.
426 A 2-tailed t-test was used for comparisons between 2 groups. A 1-way ANOVA followed by the
427 Holm-Sidak method of multiple comparisons was used for comparisons of more than 2 groups.
428 A p value of < 0.05 was considered significant.

429 **Study approval**

430 All in-house animal studies were reviewed by, approved by, and performed in compliance with
431 Alector's Institutional Animal Care and Use Committee protocols. Outsourced studies were

432 conducted in accordance with the applicable Covance or Charles River Laboratories standard
433 operating procedures, which approved these studies.

434

435 **Supplementary Materials**

436 **Supplementary Materials and Methods**

437 **Activation of myeloid cells by Siglecs**

438 The ability of different Siglec family members to reprogram MDSCs was evaluated. The ECDs
439 of Siglec-3, -5, -7, -9, and -10 were expressed as mouse IgG1 fusion proteins and incubated with
440 human MDSCs for 48 hours. Flow cytometry to assess cell surface molecules and analysis of
441 conditioned media for chemokines were performed.

442

443 **Supplementary Figures**

444 Fig. S1. Siglec-9-Fc demonstrated binding of a variety of sialic acid ligands.

445 Fig. S2. Siglec-9-Fc has a unique impact on MDSC activation and suppression markers.

446 Fig. S3. Siglec-9-Fc induced CCL4 production by MDSCs.

447 Fig. S4. AL009 relieved MDSC-mediated suppression of T cells with an EC_{50} of 1-2 nM.

448 Fig S5. AL009 induced dose-dependent increases in CD86 on monocytes.

449

450 **References**

451 1. P. R. Crocker, J. C. Paulson, A. Varki, Siglecs and their roles in the immune system. *Nat.*
452 *Rev. Immunol.* **7**, 255-266 (2007).
453 2. H. Laubli, A. Varki, Sialic acid-binding immunoglobulin-like lectins (Siglecs) detect self-
454 associated molecular patterns to regulate immune responses. *Cell. Mol. Life Sci.* **77**, 593-
455 605 (2020).
456 3. J. S. Dos Reis, I. Diniz-Lima, M. Santos, P. M. Barcelos, K. M. da Costa, R. D. C.
457 Valente, L. S. Chaves, L. P. de Campos, A. C. Dos Santos, R. G. Correia de Lima, D.
458 Decote-Ricardo, A. Morrot, J. O. Previato, L. Mendonca-Previato, C. G. Freire-de-Lima,
459 L. M. D. Fonseca, L. Freire-de-Lima, The blessed union of glycobiology and
460 immunology: A marriage that worked. *Medicines (Basel)* **10**, (2023).
461 4. M. S. Macauley, P. R. Crocker, J. C. Paulson, Siglec-mediated regulation of immune cell
462 function in disease. *Nat. Rev. Immunol.* **14**, 653-666 (2014).
463 5. K. C. M. Santegoets, P. R. Gielen, C. Bull, B. M. Schulte, E. D. Kers-Rebel, B. Kusters,
464 S. Bossman, M. Ter Laan, P. Wesseling, G. J. Adema, Expression profiling of immune
465 inhibitory Siglecs and their ligands in patients with glioma. *Cancer Immunol.*
466 *Immunother.* **68**, 937-949 (2019).
467 6. J. C. Paulson, M. S. Macauley, N. Kawasaki, Siglecs as sensors of self in innate and
468 adaptive immune repsonses. *Ann. N. Y. Acad. Sci.* **1253**, 37-48 (2012).
469 7. E. Rodriguez, S. T. T. Schetters, Y. van Kooyk, The tumour glyco-code as a novel
470 immune checkpoint for immunotherapy. *Nat. Rev. Immunol.* **18**, 204-211 (2018).
471 8. H. Laubli, S. C. Nalle, D. Maslyar, Targeting the Siglec-Sialic acid immune axis in
472 cancer: Current and future approaches. *Cancer Immunol. Res.* **10**, 1423-1432 (2022).

473 9. G. Murugesan, B. Weigle, P. R. Crocker, Siglec and anti-Siglec therapies. *Curr. Opin.*
474 *Chem. Biol.* **62**, 34-42 (2021).
475 10. A. N. Orekhov, V. A. Orekhova, N. G. Nikiforov, V. A. Myasoedova, A. V. Grechko, E.
476 B. Romanenko, D. Zhang, D. A. Chistiakov, Monocyte differentiation and macrophage
477 polarization. *Vessel Plus* **3**, 10 (2019).
478 11. J. Zhou, Z. Tang, S. Gao, C. Li, Y. Feng, X. Zhou, Tumor-associated macrophages:
479 recent insights and therapies. *Front. Oncol.* **10**, 188 (2020).
480 12. V. Kumar, S. Patel, E. Tcyganov, D. I. Gabrilovich, The nature of myeloid-derived
481 suppressor cells in the tumor microenvironment. *Trends Immunol.* **37**, 208-220 (2016).
482 13. Y. Chen, Y. Song, W. Du, L. Gong, H. Chang, Z. Zou, Tumor-associated macrophages:
483 An accomplice in solid tumor progression. *J. Biomed. Sci.* **26**, 78 (2019).
484 14. M. Lv, X. Zhuang, S. Shao, X. Li, Y. Cheng, D. Wu, X. Wang, T. Qiao, Myeloid-derived
485 suppressor cells and CD68(+)CD163(+)M2-like macrophages as therapeutic response
486 biomarkers are associated with plasma inflammatory cytokines: A preliminary study for
487 non-small cell lung cancer patients in radiotherapy. *J. Immunol. Res.* **2022**, 3621496
488 (2022).
489 15. H. Cai, Y. Zhang, J. Wang, J. Gu, Defects in macrophage reprogramming in cancer
490 therapy: The negative impact of PD-L1/PD-1. *Front. Immunol.* **12**, 690869 (2021).
491 16. S. Q. Qiu, S. J. H. Waaijer, M. C. Zwager, E. G. E. de Vries, B. van der Vegt, C. P.
492 Schroder, Tumor-associated macrophages in breast cancer: Innocent bystander or
493 important player? *Cancer Treat. Rev.* **70**, 178-189 (2018).

494 17. N. Xiao, X. Zhu, K. Li, Y. Chen, X. Liu, B. Xu, M. Lei, J. Xu, H. C. Sun, Blocking
495 siglec-10(hi) tumor-associated macrophages improves anti-tumor immunity and enhances
496 immunotherapy for hepatocellular carcinoma. *Exp. Hematol. Oncol.* **10**, 36 (2021).
497 18. Z. Duan, Y. Luo, Targeting macrophages in cancer immunotherapy. *Signal Transduct.*
498 *Target Ther.* **6**, 127 (2021).
499 19. M. Viitala, R. Virtakoivu, S. Tadayon, J. Rannikko, S. Jalkanen, M. Hollmen,
500 Immunotherapeutic blockade of macrophage clever-1 reactivates the CD8(+) T-cell
501 response against immunosuppressive tumors. *Clin. Cancer Res.* **25**, 3289-3303 (2019).
502 20. A. M. Georgoudaki, K. E. Prokopec, V. F. Boura, E. Hellqvist, S. Sohn, J. Ostling, R.
503 Dahan, R. A. Harris, M. Rantalainen, D. Klevebring, M. Sund, S. E. Brage, J. Fuxe, C.
504 Rolny, F. Li, J. V. Ravetch, M. C. Karlsson, Reprogramming tumor-associated
505 macrophages by antibody targeting inhibits cancer progression and metastasis. *Cell Rep.*
506 **15**, 2000-2011 (2016).
507 21. L. La Fleur, J. Botling, F. He, C. Pelicano, C. Zhou, C. He, G. Palano, A. Mezheyeuski,
508 P. Micke, J. V. Ravetch, M. C. I. Karlsson, D. Sarhan, Targeting MARCO and IL37R on
509 immunosuppressive macrophages in lung cancer blocks regulatory T cells and supports
510 cytotoxic lymphocyte function. *Cancer Res.* **81**, 956-967 (2021).
511 22. A. Mantovani, P. Allavena, F. Marchesi, C. Garlanda, Macrophages as tools and targets
512 in cancer therapy. *Nat. Rev. Drug Discov.* **21**, 799-820 (2022).
513 23. G. Genard, S. Lucas, C. Michiels, Reprogramming of tumor-associated macrophages
514 with anticancer therapies: radiotherapy versus chemo- and immunotherapies. *Front.*
515 *Immunol.* **8**, 828 (2017).

516 24. H. Benonisson, H. S. Sow, C. Breukel, J. Claassens, C. Brouwers, M. M. Linssen, M. F.
517 Fransen, M. Sluijter, F. Ossendorp, T. van Hall, J. S. Verbeek, High FcgammaR
518 expression on intratumoral macrophages enhances tumor-targeting antibody therapy. *J.*
519 *Immunol.* **201**, 3741-3749 (2018).
520 25. A. Haslam, V. Prasad, Estimation of the percentage of US patients with cancer who are
521 eligible for and respond to checkpoint inhibitor immunotherapy drugs. *JAMA. Netw.*
522 *Open.* **2**, e192535 (2019).
523 26. P. Pathria, T. L. Louis, J. A. Varner, targeting tumor-associated macrophages in cancer.
524 *Trends Immunol.* **40**, 310-327 (2019).
525 27. N. Kumari, S. H. Choi, Tumor-associated macrophages in cancer: recent advancements in
526 cancer nanoimmunotherapies. *J. Exp. Clin. Cancer Res.* **41**, 68 (2022).
527 28. X. Xiang, J. Wang, D. Lu, X. Xu, Targeting tumor-associated macrophages to synergize
528 tumor immunotherapy. *Signal Transduct. Target Ther.* **6**, 75 (2021).
529

530 **Acknowledgments:** Editorial support and publication assistance were provided by SCIENT
531 Healthcare Communications (Cedar Knolls, NJ, USA).

532 **Funding:** All studies were supported by Alector, Inc.

533 **Author contributions:**

534 Conceptualization: SCN, SL, AR

535 Investigation: SCN, HL, LL

536 Analysis: SCN, HL, LL

537 Writing – original draft: SCN, DM

538 Writing – review and editing: SCN, DM

539 **Competing interests:** All authors are shareholders of Alector, Inc., or were shareholders of

540 Alector, Inc., when the studies were being conducted. SCN and SL are inventors on a patent

541 application related to this work.

542 **Data and materials availability:**

543 All data are available in the main text or supplementary materials.